Zero : Jurnal Sains, Matematika, dan Terapan
E-ISSN : 2580-5754; P-ISSN : 2580-569X
Volume 9, Number 2, 2025
DOI: 10.30829/zero.v9i2.26192
Page: 600-611

Data-Efficient LSTM Modeling for Climate-based Dengue Early Warning in Lampung, Indonesia

[1] **Rifky Fauzi**
Department of Mathematics, Institut Teknologi Sumatera, Lampung Selatan, 35365, Indonesia

[2] **Mia Syntia Br Sinaga**
Department of Mathematics, Institut Teknologi Sumatera, Lampung Selatan, 35365, Indonesia

[3] **Nela Rizka**
Department of Mathematics, Institut Teknologi Sumatera, Lampung Selatan, 35365, Indonesia

[4] **Dear Michiko Mutiara Noor**
Department of Mathematics, Institut Teknologi Sumatera, Lampung Selatan, 35365, Indonesia

[5] **Aswan Anggun Pribadi**
Department of Mathematics, Institut Teknologi Sumatera, Lampung Selatan, 35365, Indonesia

[6] **Tiara Shofi Edriani**
Department of Mathematics, Institut Teknologi Sumatera, Lampung Selatan, 35365, Indonesia

Article Info

Article history:

Accepted, 30 October 2025

Keywords:

Climate factors;
Data efficiency;
Dengue forecasting;
Early warning system;
LSTM.

ABSTRACT

We present a data-efficient recurrent framework for climate-informed dengue early warning in Lampung Province. Monthly incidence and climate records are transformed into supervised sequences with 2–3-month lags, consistent with the observed lead–lag structure. Three architectures i.e. single-layer LSTM, stacked LSTM, and Temporal-Attention LSTM (TA-LSTM) are tuned via a compact genetic search under a time-ordered split. Performance improves with longer history; the TA-LSTM (37 units) attains the best accuracy. Permutation feature importance reveals a clear hierarchy: relative humidity and maximum temperature dominate, autoregressive incidence contributes moderately, while rainfall, sunshine, and minimum temperature are secondary; average temperature is largely redundant. The findings indicate that adding meaningful historical context and selective temporal weighting yields robust early-warning capability from coarse, time-limited data, and that humidity–temperature dynamics, together with short-term incidence persistence, are the principal drivers in this provincial setting.

Corresponding Author:
Tiara Shofi Edriani,
Department of Mathematics, Faculty of Sciences
Institut Teknologi Sumatera
Email: tiara.edriani@ma.itera.ac.id

1. INTRODUCTION

Dengue fever (DF) is one of the most prevalent mosquito-borne viral diseases in tropical and subtropical regions and continues to pose a major global public health threat [1]. The disease is caused by the dengue virus,

which is transmitted through the bites of infected female *Aedes aegypti* and *Aedes albopictus* mosquitoes. In 2019, dengue was listed by the World Health Organization as one of the ten greatest global health threats, and the number of cases reported in 2023 reached the highest level recorded to date [2]. This persistent burden underscores the strong linkage between dengue transmission dynamics and environmental variability, particularly climate change.

The primary vector, *Aedes aegypti*, is highly sensitive to climatic conditions such as temperature, rainfall, and relative humidity. These factors influence the mosquito's life cycle and the efficiency of viral replication and transmission. Temperature accelerates mosquito development and viral incubation [3],[4], while humidity supports adult survival and increases biting frequency. Rainfall determines the availability of breeding sites, directly affecting larval density and vector abundance[5], [6], [7]. Consequently, climatic fluctuations exert a considerable impact on dengue incidence, both through short-term weather anomalies and longer-term climate patterns.

Empirical studies have shown that optimal humidity levels (66.67%–89.6%) are associated with an increase in dengue cases, often preceded by periods of intense rainfall or the onset of the wet season [8]. These climatic factors not only regulate mosquito reproduction and longevity but also influence the timing and intensity of dengue outbreaks. However, the effects of climate conditions are not immediate; rather, they are delayed due to the biological processes governing mosquito development and virus transmission. This delay—commonly referred to as the *time lag effect*—represents the period between changes in climatic variables and their observable impact on dengue incidence [9], [10], [11]. Considering this lag is essential for improving disease prediction accuracy, as climatic variations typically require several weeks to translate into measurable changes in case counts.

Previous climate-based dengue models in Indonesia have primarily focused on metropolitan or coastal regions such as Jakarta [12] and Bali [13], where high-resolution datasets and long-term surveillance records are available. For example, studies such as DBDKlim successfully integrated climatic predictors into early-warning frameworks for those areas. In contrast, Lampung Province—despite being a key endemic region in southern Sumatra—has not yet been systematically analyzed using data-driven predictive approaches that incorporate lagged climate factors. This absence of localized modeling limits the capacity to design timely public health interventions in the province.

To address this research gap, the present study applies Long Short-Term Memory (LSTM) neural networks to explore the delayed influence of climatic variables on dengue incidence in Lampung Province, Indonesia. LSTM, a variant of recurrent neural networks specifically designed to capture long-term temporal dependencies in sequential data [14], provides a robust framework for modeling the nonlinear and lagged relationships between weather fluctuations and disease transmission patterns. By explicitly incorporating lagged climatic predictors including temperature, rainfall, relative humidity, and Dengue incidence. The model seeks to better represent the incubation-related delays inherent in dengue transmission dynamics.

Unlike previous works that primarily focused on national or city-level models such as the DBDKlim systems in Jakarta and Bali, this study represents the first localized data-driven modeling effort for Lampung Province. It introduces a data-efficient framework that integrates empirically derived lag structures, Long Short-Term Memory (LSTM) networks, and Genetic Algorithm (GA)-based optimization to enhance predictive reliability under limited and aggregated provincial data conditions. Because both climate and dengue data are recorded monthly and often subject to reporting delays, the most recent month's information is typically incomplete at the time of forecasting. Therefore, this study focuses on 2–3-month lagged predictors, representing the most operationally reliable and biologically relevant time window for early warning. The purpose of this research is to develop an efficient and interpretable deep learning model capable of providing a climate-based dengue early warning system for Lampung, Indonesia. This framework highlights innovation in combining data efficiency, temporal depth, and automatic optimization to strengthen early disease surveillance in data-limited regions.

2. RESEARCH METHOD

2.1. Study Area

Lampung Province lies at the southernmost part of Sumatra Island, Indonesia, between 3°45′–6°45′ S and 103°40′–105°50′ E. The province covers approximately 35,000 km² and has a tropical monsoon climate characterized by two distinct seasons: a wet season from November to April and a dry season from May to October. Average monthly temperatures range between 24 °C and 33 °C, with annual rainfall exceeding 2500 mm in several districts. Major urban centers such as Bandar Lampung, Metro, and Pringsewu record recurrent dengue outbreaks each year. Although dengue surveillance has been continuously conducted by the local health authorities, no previous data-driven climatic prediction system has been developed for the region—unlike the DBDKlim initiatives implemented in Jakarta and Bali. This research therefore represents the first systematic attempt to construct a localized LSTM-based climate–dengue forecasting framework for Lampung.

2.2. Data Description

This study is designed to support government decision-making by optimizing the existing data ecosystem available within provincial institutions. Monthly dengue incidence data from January 2015 to September 2024 were obtained from the Lampung Provincial Health Office and standardized per 100,000 population using interpolated mid-year census data from the Indonesian Bureau of Statistics (BPS). The data are aggregated at the

provincial level, reflecting the official reporting structure in which dengue surveillance is compiled and verified monthly before publication. Although such aggregation may reduce sensitivity to local outbreak variations, it provides a realistic and operational foundation for developing predictive models based on the data infrastructure currently accessible to regional authorities. Climatic predictors i.e. average temperature (°C), total rainfall (mm), and relative humidity (%) were obtained from the Meteorological, Climatological, and Geophysical Agency (BMKG), derived from validated local stations and sensor networks that ensure robust and complete monthly coverage. Both climate and dengue datasets were complete, with no missing values.

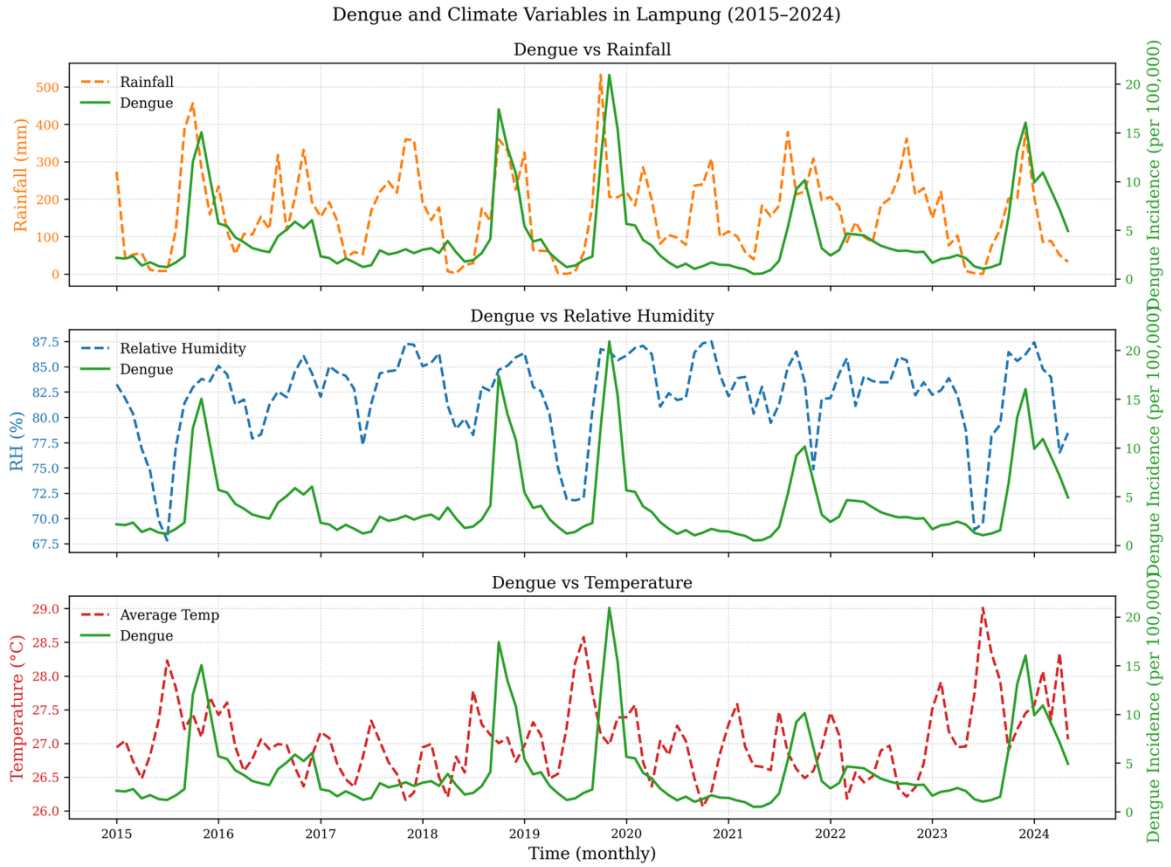

Figure 1. Dengue incidence and climate data in Lampung (2015–2024).

Figure 1 overlays monthly dengue incidence (indicated by right y-axis) with three climate variables (indicated by left y-axis) from Jan-2015 to 2024. In the rainfall data, major dengue surges (e.g., early-2016, late-2019/early-2020, and 2024) occur shortly after large rainfall peaks, suggesting a lagged, positive association consistent with increased vector breeding following wet months. The relative humidity data shows dengue tending to rise during periods of sustained higher RH (approximately 80–85%), again with a short delay, troughs in RH coincide with relatively lower dengue. The Temperature data exhibits a weaker pattern i.e. temperature varies within a narrow band (approximately 26–28.5 °C), and dengue peaks visually do not align as tightly with short-term temperature fluctuations as they do with rainfall and humidity. Overall, the plots indicate stronger seasonality and lagged co-movement of dengue with rainfall and humidity than with temperature, motivating formal lagged or distributed-lag modeling in the analysis.

Dengue transmission is highly localized and influenced by specific climatic variables (temperature, rainfall, humidity) that can vary significantly between regions [15], [16]. A model trained on the climate–dengue relationship in one area might not accurately capture the nuances in another. The unique characteristics of each region's climate patterns, mosquito populations (vector species, density, breeding sites), and human population density all contribute to the localized nature of dengue outbreaks. For this reason, the present study focuses specifically on Lampung Province, a dengue-endemic region in southern Sumatra, to capture its regional climatic and epidemiological signatures. While the analysis evaluates model performance through internal train–test validation, external regional validation remains a future direction once standardized multi-provincial datasets become available. Overall, this approach demonstrates how data-efficient deep learning can extract reliable early-warning signals from aggregated, limited-resolution data, aligning computational innovation with the practical realities of public health surveillance in Indonesia.

2.3. Data Pre-processing

Prior to model development, all variables were synchronized to a common monthly timeline. Missing climate observations (< 2 %) were linearly interpolated. Each feature was then normalized to the range [0, 1] using a Min–Max scaler fitted exclusively on the training subset to prevent data leakage. To reflect the temporal dependency of dengue transmission, input–output sequences were structured in a sliding-window format: for each month t, the previous p months of climate data were used to predict dengue incidence at $t + 1$. Lag selections of $p = 1 - 6$ were compared during model tuning. The full dataset was divided chronologically into training (80 %), and testing (20 %) sets, ensuring that future information did not leak into earlier periods. Performance stability was further checked using a rolling-origin cross-validation scheme.

2.4. Model Architecture

LSTM cells as computational unit

An LSTM processes a sequence month-by-month and maintains an internal memory that decides what information should be kept or forgotten. At each time step, three gates—forget, input, and output—control how much of the past is retained and how much of the new signal is incorporated. This gating mechanism allows the LSTM to overcome the vanishing-gradient problem and capture delayed climatic effects on dengue incidence, such as rainfall or humidity influences that appear 2–3 months later. In the standard formulation, only the final hidden state h_L is used to produce the prediction, which means all earlier months influence the output only indirectly through the LSTM memory.

The Long Short-Term Memory (LSTM) network is a variant of the Recurrent Neural Network (RNN) designed to overcome the *vanishing gradient* problem commonly encountered in sequential or time-series data processing. Unlike conventional RNNs, which tend to lose information over long sequences, the LSTM architecture can selectively retain, update, and discard information across extended time spans, allowing it to capture complex temporal dependencies among variables in time-series datasets [17].

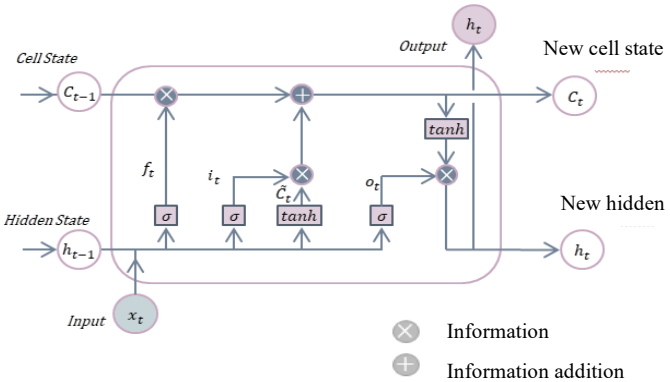

Figure 2. Illustration of an LSTM Cell

An LSTM network consists of a series of processing units known as *memory cells* (Figure 2), each containing three main gates: the forget gate, input gate, and output gate. The forget gate determines which information from the previous state should be discarded; the input gate regulates which new information should be stored in the cell; and the output gate controls which portion of the cell state is passed forward as the hidden output [18]. Through these mechanisms, the LSTM can maintain long-term dependencies in the data more stably and effectively than a standard RNN.

Mathematically, the internal structure of the LSTM cell can be described as follows.

(a) Forget Gate decides what portion of the previous information should be retained or discarded, based on the current input x_t and the previous hidden state h_{t-1}

$$\sigma(W_f \cdot [h_{t-1}, x_t] + b_f)$$

where f_t is the forget gate vector at time t, x_t is the input, h_{t-1} is the previous hidden state, W_f and b_f are the weight and bias terms, and σ denotes the sigmoid activation function.

(b) Input Gate regulates the information to be added to the current cell state using two activation functions (sigmoid and *tanh*):

$$i_t = \sigma(W_i[h_{t-1}, x_t] + b_i)$$
$$\widetilde{C_t} = \tanh(W_c \cdot [h_{t-1}, x_t] + b_c)$$

where i_t represents the input gate, $\widetilde{C_t}$ is the candidate cell state, W_i and W_c are the respective weight matrices, b_i and b_c are the bias vectors, and *tanh* is the hyperbolic tangent activation.

(c) Cell State Update combines the retained information from the forget gate and the new candidate state to update the overall memory cell

$$C_t = f_t \cdot C_{t-1} + i_t \cdot \widetilde{C}_t$$

where C_t and C_{t-1} denote the current and previous cell states, respectively.

(d) Output Gate determines the next hidden state h_t that serves as both the output and the recurrent input for the next time step

$$o_t = \sigma(W_o \cdot [h_{t-1}, x_t] + b_o)$$
$$h_t = o_t \cdot \tanh(C_t)$$

In this study, the LSTM model is applied to predict dengue incidence by learning the temporal relationships between rainfall, humidity, temperature, and sunshine duration and the monthly number of dengue cases. By incorporating time-lagged climate variables, the LSTM can detect delayed effects between environmental fluctuations and subsequent increases in dengue incidence, leading to more precise forecasting for disease monitoring and control [19].

Time Attention Mechanism

While the LSTM can store long-range information, relying only on its final hidden state means earlier months may be overshadowed or lost during the update process. Temporal attention addresses this limitation by allowing the model to assign different importance levels to each month in the input window. Instead of treating all past observations equally, the attention mechanism learns which months are most relevant. By combining the entire sequence of LSTM outputs using data-driven importance weights, the attention layer highlights the key historical periods that contribute most to the next month's dengue incidence, improving both prediction accuracy and interpretability.

Let an input window $\mathrm{X} = (x_1, \ldots, x_L)$, $\mathrm{x}_t \in \mathbb{R}^d$. An LSTM encodes the sequence into hidden states $\mathrm{h}_t \in \mathbb{R}^H$ (and cells c_t), e.g.

$$\begin{aligned} i_t &= \sigma(W_i x_t + U_i h_{t-1} + b_i), \quad & f_t &= \sigma(W_f x_t + U_f h_{t-1} + b_f), \\ \tilde{c}_t &= \tanh(W_c x_t + U_c h_{t-1} + b_c), \quad & c_t &= f_t \odot c_{t-1} + i_t \odot \tilde{c}_t, \\ o_t &= \sigma(W_o x_t + U_o h_{t-1} + b_o), \quad & h_t &= o_t \odot \tanh(c_t). \end{aligned}$$

Instead of using only the last state h_L, temporal attention learns data-driven weights over all $\{\mathrm{h}_t\}_{t=1}^{L}$ and forms a context vector c by a convex combination:

$$c = \sum_{t=1}^{L} \alpha_t h_t, \quad \alpha_t = \frac{exp\,(e_t)}{\sum_{j=1}^{L} exp\,(e_j)}, \quad \alpha_t \geq 0, \quad \sum_t \alpha_t = 1$$

The vector e_t measures how relevant h_t is for the current prediction. Two common choices:

i. Additive attention

$$e_t = \mathrm{v}^\top \tanh\big(W_h h_t + W_q q + b\big),$$

where v is also trainable weight representing which accumulates the transformed hidden states.

ii. Dot-product attention

$$e_t = \frac{1}{\sqrt{H}}\, \mathrm{h}_t^\top \mathrm{q}.$$

Here the query q summarizes "what the model currently needs." In sequence forecasting, a standard and effective choice is

$$\mathrm{q} = W_c\, \mathrm{h}_L \quad \text{(query derived from the last LSTM state)},$$

though q can also be a learned vector or another function of $\{\mathrm{h}_t\}$. Finally, the model predicts from c (optionally concatenated with h_L):

$$\hat{y} = W_y\, \mathrm{c} + b_y$$

The weights α_t are time-step importances, large α_t means the model relies more on month t in the look-back window. Because α_t form a probability simplex, the mechanism yields an interpretable, normalized attribution over past times. Training minimizes a loss (e.g., MSE) and backpropagates through the softmax, jointly learning the encoder (LSTM) and the attention scorer (W_h, W_q, v, ...).

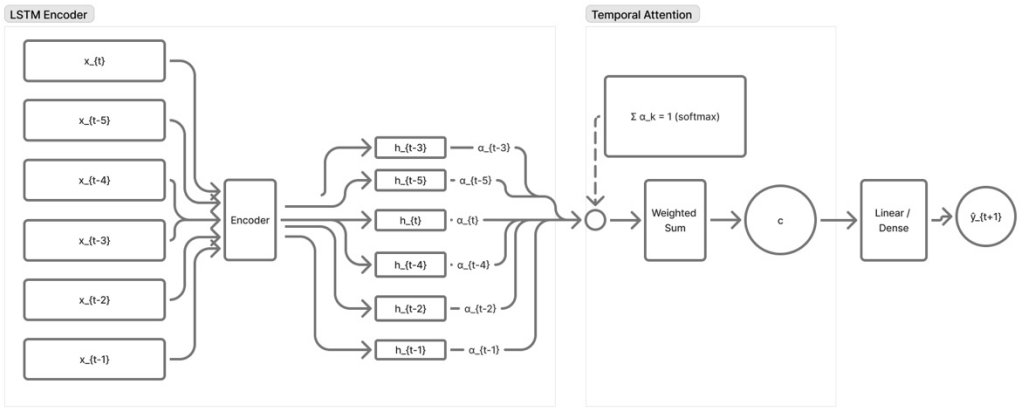

Figure 3. Temporal Attention Mechanism in the LSTM

In Figure 3, The attention mechanism enhances the interpretability and performance of the LSTM by allowing the model to focus selectively on key historical time steps instead of treating all past data equally. In dengue–climate forecasting, climatic effects (e.g., rainfall or temperature) often influence dengue incidence with 2–3 month lags due to mosquito life cycles and virus incubation periods. The attention weights α_t quantify these delayed effects dynamically, enabling the model to prioritize the most impactful months automatically. Thus, while the LSTM captures overall temporal dependencies, the attention layer adaptively highlights which lag intervals contribute most to the current outbreak, improving both accuracy and interpretability in early-warning applications.

Proposed LSTM Architecture

Figure 3 compares three sequence-modeling pipelines used for one-step-ahead dengue prediction from a look-back window of monthly observations. All variants share the same input and output scaffold: the input sequence is first normalized with Batch Normalization to stabilize training; the final prediction is produced by a linear Dense head, with Dropout before the head for regularization. The LSTM baseline (left) uses a single recurrent layer whose last hidden state summarizes the window. The Stacked LSTM (center) deepens the temporal encoder by feeding a second LSTM with the full sequence of states from the first, enabling higher-order temporal interactions. The LSTM + Temporal Attention model (right) retains the full sequence of LSTM states, applies Spatial Dropout (channel-wise) as stronger regularization, and then a Temporal Attention block that learns importance weights over past months to form a context vector, from which the Dense head predicts the next value. This design isolates the effects of depth (Stacked LSTM) and data-driven time weighting (Attention) while keeping preprocessing and heads identical.

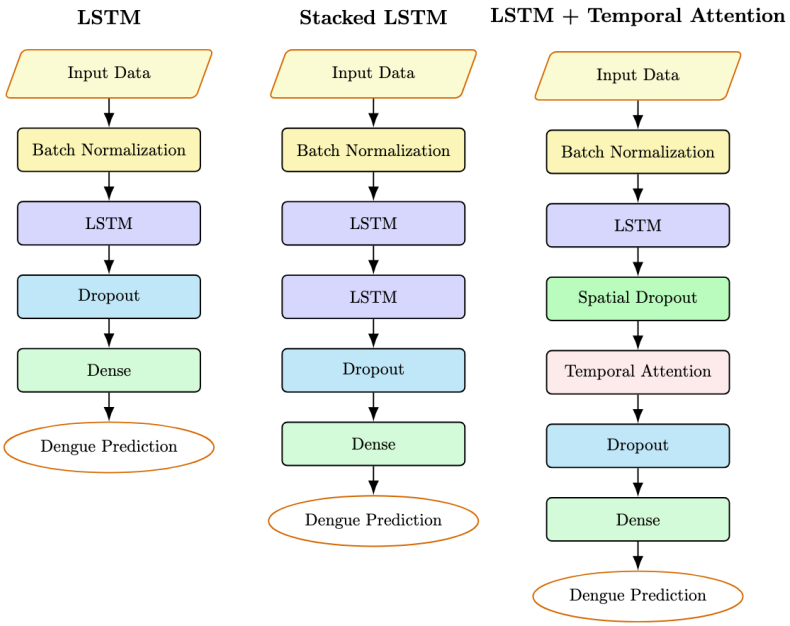

Figure 4. Architectures evaluated for dengue prediction—(left) LSTM, (center) Stacked LSTM, and (right) LSTM with Temporal Attention. Each pipeline receives an input sequence, applies batch normalization, encodes with one or two LSTMs, regularizes (dropout), and predicts through a dense layer; the attention model additionally learns per-time-step weights before the prediction head

2.5. Benchmark and Evaluation

Model performance was evaluated using Mean Absolute Percentage Error (MAPE), Mean Absolute Error (MAE), Root Mean Squared Error (RMSE), and the coefficient of determination (R^2). Lower error values and higher R^2 indicate better predictive accuracy.

The Mean Absolute Percentage Error (MAPE) is expressed as

$$MAPE = \frac{100\%}{N}\sum_{t-1}^{N}\frac{|y_t - \hat{y}_t|}{|y_t|}$$

where y_t represents the actual value at time t, $\hat{y}_t$ denotes the predicted value at time t, and N is the total number of observations.

MAPE quantifies the average prediction error as a percentage, thereby providing an intuitive measure of how far predicted values deviate from the observed data. The interpretation of MAPE values is summarized in Table 1.

Table 1. Range MAPE values [20]

Range MAPE	Interpretation
$MAPE \leq 10\%$	Highly accurate forecasting
$10\% < MAPE \leq 20\%$	Good forecasting
$20\% < MAPE \leq 50\%$	Reasonable forecasting
$MAPE > 50\%$	Inaccurate forecasting

Meanwhile, the Mean Squared Error (MSE) is employed as the loss function during model training, as it imposes a larger penalty on greater deviations, thereby guiding the model to minimize the difference between predicted and actual values. The MSE is defined as [20]:

$$MSE = \frac{1}{n}\sum_{i=1}^{n}(y_t - \hat{y}_t)^2$$

$$RMSE = \left(\frac{1}{n}\sum_{i=1}^{n}(y_t - \hat{y}_t)^2\right)^{1/2}$$

where y_i denotes the actual value at the i-th observation, $\hat{y}_i$ is the corresponding predicted value, and N represents the total number of observations. The loss function used in this study is MSE i.e. equation 9. This loss is applied throughout the training process to update the neural network's weights.

2.6. Genetic Algorithm for Hyper-parameter Tuning

To select the hyper-parameters of each LSTM variant (number of cells per layer, and when applicable both layers). Each candidate solution is an integer vector of hyper-parameters θ(e.g., $\theta = [u_1]$for one LSTM layer or $\theta = [u_1, u_2]$for a stacked model). A population of such candidates is evolved across generations. For a given θ, we train the model on the inner training split with early stopping and evaluate the validation RMSE as fitness; lower is better. In each generation we (i) keep a small set of elites (best candidates), (ii) create offspring by selection (tournament or probability proportional to quality), crossover (per-gene mixing from two parents), and mutation (small random integer steps with clipping to bounds), and (iii) repeat until a fixed number of generations or convergence. The best $\boldsymbol{\theta}$ is then retrained on (almost) the full training data and finally evaluated on the held-out test block.

Let $\mathcal{P}^{(t)} = \{\boldsymbol{\theta}_i^{(t)}\}_{i=1}^{N}$ be the population at generation t.

Fitness

The fitness function can be any real valued function depending on the problem. For this case of Dengue prediction we will minimize the RMSE of the prediction i.e. equation 10.

Selection

With quality $q_i^{(t)} = \frac{1}{f(\boldsymbol{\theta}_i^{(t)})}$, select parent indices with

$$p_i^{(t)} = \frac{q_i^{(t)}}{\sum_{k=1}^{N} q_k^{(t)}}, \text{Parent} \sim \text{Categorical}(p_1^{(t)}, \dots, p_N^{(t)}),$$

(or tournament selection in practice).

Crossover

For parents $\boldsymbol{\theta}_a, \boldsymbol{\theta}_b$and Bernoulli mask $\mathbf{m} \in \{0,1\}^d$,

$$\boldsymbol{\theta}_{\text{child}} = \mathbf{m} \odot \boldsymbol{\theta}_a + (\mathbf{1} - \mathbf{m}) \odot \boldsymbol{\theta}_b.$$

Mutation

$$\tilde{\boldsymbol{\theta}} = \boldsymbol{\theta}_{\text{child}} + s\,\boldsymbol{\xi}, \xi_k \in \{-2,-1,1,2\} \text{ with prob. } \rho, \text{ else } 0,$$

for each component k,

$$\theta'_k = \min\left(\max\left(\tilde{\theta}_k, \ell_k\right), u_k\right).$$

If mutation pushes below ℓ_k, it's set to ℓ_k; if it exceeds u_k, it's set to u_k. Where $\boldsymbol{\ell}, \boldsymbol{u}$ are lower/upper bounds (e.g., units $\in [8,128]$) and $s$is the step size (e.g., multiples of 8 cells).

Elitism and next generation

Let $\mathcal{P}_t = \{\boldsymbol{\theta}_1^{(t)}, \ldots, \boldsymbol{\theta}_N^{(t)}\}$ be the size-N population of candidate hyper-parameters at generation t. The update

$$\mathcal{P}_{t+1} = \text{Top}_K(\mathcal{P}_t) \cup \text{Children}_{N-K}$$

Stopping

Stop when $t = T_{\max}$or when

$$\min_{\boldsymbol{\theta}\in\mathcal{P}^{(t)}} f(\boldsymbol{\theta}) \text{ fails to improve by more than } \varepsilon \text{ for } G \text{ generations.}$$

This GA framework yields, for each combination of number of cells for each architecture (LSTM, Stacked LSTM, LSTM+Attention), a data-driven choice of the number of cells that minimizes validation RMSE while respecting integer/bounded constraints.

3. RESULT AND ANALYSIS

3.1 Lead–Lag Structure between Climate and Dengue

We quantify how far in advance climate signals anticipate dengue by computing Pearson cross-correlations between current Dengue incidence and (i) Dengue incidence past values and (ii) lagged rainfall, relative humidity, and average temperature at 2 and 3 months. Incidence is moderately persistent at 2 months ($r \approx 0.36^*$) but largely fades by 3 months. Rainfall shows a clear positive link at 2 months ($r \approx 0.36^*$), while average temperature is positively associated at both 2 and 3 months ($r \approx 0.33^*, 0.57^*$). Relative humidity is weak at 2 months and negative at 3 months ($r \approx -0.29^*$). The asterisks symbol denote significance for $p < 0.05$.

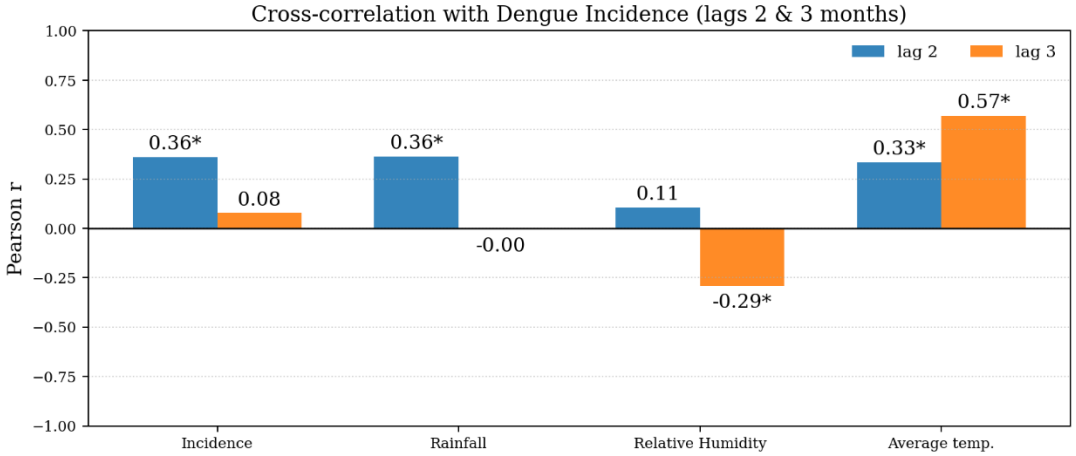

Figure 5. Cross-correlation of current dengue incidence with incidence (autocorrelation), rainfall, relative humidity, and average temperature at lags of 2 and 3 months for 2015–2024 (asterisks indicate statistical significance at p<0.05)

Ecologically, these patterns are consistent with Dengue vector, i.e. Aedes dynamics. Heavy rain creates breeding sites; allowing for larval development, adult emergence, virus extrinsic incubation, and reporting delays yields a compounded lag near 2 months. Warmer conditions accelerate development, biting, and viral replication, sustaining an effect out to 3 months. The negative relative humidity at 3 months likely reflects seasonal transitions and behavior (e.g., pre-rainfall water storage increasing container habitats) and/or collinearity with rainfall—hence it should be interpreted within a multivariate, distributed-lag model rather than as an isolated causal driver. Overall, the 2–3-month lead in rainfall and average temperature supports their use in early-warning systems.

3.2 Genetic Algorithm Settings for Hyperparameter Tuning

We tuned the number of LSTM units for three models—(i) LSTM, (ii) Stacked LSTM, and (iii) LSTM with Attention. Data were split in time (80% train, 20% test). From the training block, the last 20% served as a validation fold used only to choose hyper-parameters. Inputs/targets were standardized using training statistics to avoid leakage. The score we minimize is the validation RMSE in equation 10. A candidate (a "chromosome") is the number of units in each LSTM layer: LSTM: (n_1), TA-LSTM: (n_1), and Stacked LSTM: (n_1, n_2). Each n_i

is an integer between 8 and 128. For a candidate, we train the model on the inner-train split with early stopping (max 50 epochs) and take its $RMSE_{val}$.

We use a small population and few generations to keep compute practical: population $P = 8$, generations $G = 5$.

1. Start with P random candidates.
2. Evaluate each: train briefly, record $RMSE_{val}$.
3. Keep the best half (elitism) and create children by mixing parent genes (single-point crossover) and randomly changing one gene with prob. 0.3(mutation).
4. Repeat steps 2–3 for G generations.

A concise update view is done by employing i.e. equation 11, the next population is the best half plus offspring from crossover+mutation. After G rounds we pick the best settings $\theta^{\star}$, refit them on (almost) all training data, and then report test RMSE.

3.3 LSTM Model Evaluation

Table 2 summarizes the comparative performance of three recurrent architectures across five training generations of GA for monthly dengue prediction in Lampung. The attention-augmented model achieved the best overall accuracy, with TA-LSTM (37 units) reaching a final RMSE of 0.6429 (Gen 5), narrowly outperforming the single-layer LSTM baseline at 0.6510 (Gen 5; 76 units) and more clearly surpassing the stacked LSTM (S-LSTM) at 0.6806 (Gen 5; 86, 51 units). All models improved from their Gen 1 baselines, though to different extents: LSTM and TA-LSTM reduced RMSE by 5.36% and 4.58%, respectively, while S-LSTM showed only a 0.67% decrease and greater inter-generation variability. The head-to-head delta at convergence indicates that temporal attention provides a measurable advantage of roughly 1.24% over a substantially wider LSTM and ≈5.5% over a deeper stacked configuration.

Table 2. Perfomance of LSTM architectures for Dengue prediction in Lampung

Model	Generation	Best RMSE	Best Parameters
LSTM	Gen 1	0.6879	[58]
	Gen 2	0.6729	[55]
	Gen 3	0.6574	[55]
	Gen 4	0.6765	[76]
	Gen 5	0.6510	[76]
	Final Best	0.6510	[76]
S-LSTM	Gen 1	0.6852	[36, 72]
	Gen 2	0.6850	[37, 68]
	Gen 3	0.6790	[42, 68]
	Gen 4	0.6878	[42, 68]
	Gen 5	0.6806	[86, 51]
	Final Best	0.6806	[86, 51]
TA-LSTM	Gen 1	0.6738	[96]
	Gen 2	0.6754	[50]
	Gen 3	0.6796	[37]
	Gen 4	0.6643	[37]
	Gen 5	**0.6429**	**[37]**
	Final Best	0.6429	[37]

These findings suggest that, under the data regime studied (local, monthly series with limited sample size), selective temporal weighting offers better capacity utilization than simply increasing width (more units) or depth (additional recurrent layers). Attention likely helps the network emphasize epidemiologically salient lags (e.g., seasonal and weather-driven delays) while down-weighting noisy periods, improving generalization without large parameter growth. By contrast, the stacked model's instability across generations hints at mild overfitting and diminished sample efficiency, consistent with small-to-medium datasets. Overall, TA-LSTM is the preferred choice for this setting; however, the incremental margin over the tuned single-layer LSTM also indicates that feature design (e.g., seasonal encodings and lagged exogenous drivers) already captures much of the predictable structure, leaving limited headroom for architectural gains alone.

Previous studies [21] showed that attention mechanisms can help LSTM models focus on the most relevant information. In our work, we apply the same idea but shift the focus on temporal attention mechanism. This allows the model to automatically highlight the most important months in the input window, making it better suited for capturing the lagged climate effects that drive dengue patterns.

The findings underscore an important insight: model simplicity coupled with automatic architecture optimization can outperform more complex attention-based designs when the dataset is region-specific and moderate in size.

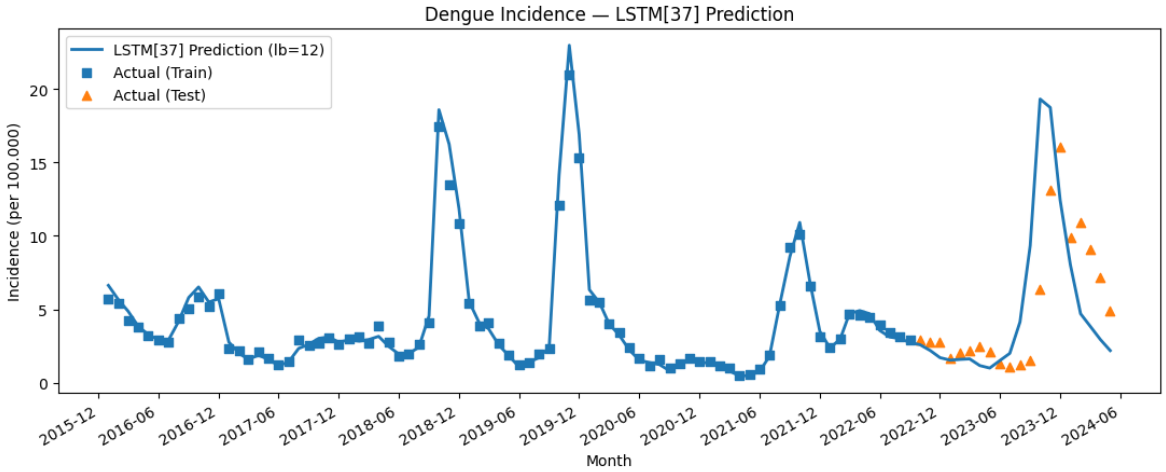

Figure 6. Monthly dengue incidence (right axis) overlaid with rainfall, relative humidity, and temperature (left axis), 2015–2024. Dengue peaks typically follow large rainfall episodes by ~1–2 months and occur during sustained high humidity (≈80–85%). Temperature fluctuates in a narrower band (≈26–28.5 °C) and shows a weaker visual alignment. These patterns motivate lagged predictors, especially for rainfall and humidity.

As shown in Figure 6, the LSTM with 37 hidden units improves systematically as the look-back horizon is lengthened, with the 12-month window recovering the province's recurrent trough–peak rhythm and the timing of seasonal upswings. Granting the network access to a full annual history exposes it to the delayed co-movement between rainfall, humidity, and incidence that characterizes Lampung, allowing its recurrent state to encode both intra-seasonal persistence and interannual modulation. The remaining discrepancy, an underestimation of the 2023–2024 crest and a slightly faster post-peak decay, reflects a conservative tendency that is typical when models are trained to be robust to outliers and rely on aggregate climate signals; timing is learned more reliably than peak amplitude in this data regime.

Methodologically, the procedure is designed for small, locality-specific surveillance data. We adopt a time-ordered train/test split to prevent information leakage and choose the look-back by minimizing the training SMAPE because no external validation set is available. The target is modeled on a logarithmic scale to stabilize variance and reduce the disproportionate influence of sporadic spikes; training emphasizes robust error penalization to prevent the fit from being dominated by a few extreme months. Inputs are standardized and lightly regularized to avoid memorization while preserving signal, and mild stochastic perturbations during training encourage the model to learn seasonally persistent features rather than noise. Together, these choices explain the behaviour in Figure 6: once additional history is provided, the LSTM capitalizes on longer-range dependencies to improve phase alignment and onset detection, while remaining deliberately cautious on unprecedented peaks, an acceptable trade-off for early-warning purposes in operational public health settings.

3.4. Feature Importance Analysis of the TA-LSTM Model

To identify which climatic and epidemiological factors most influenced the Temporal-Attention LSTM (TA-LSTM, 37 units), a Permutation Feature Importance (PFI) test was performed on the test dataset. This procedure involved randomly permuting one feature at a time to break its temporal alignment with dengue incidence while keeping all other inputs fixed. The resulting degradation in prediction accuracy, measured through changes in RMSE, and R^2, reflects how strongly the model depends on that feature. A larger increase in RMSE (positive Δ) and a decrease in R^2 (negative Δ) indicate a more influential feature. Conversely, near-zero or negative Δ values imply redundancy or weak contribution.

Table 3. Aggregated permutation feature importance of TA-LSTM model across major climatic and epidemiological variable groups

Variable	ΔRMSE	Δ R^2	Relative Influence
Relative Humidity (RH)	+0.66	−0.23	High
Maximum Temperature (Tx)	+0.57	−0.20	High
Autoregressive Incidence	+0.26	−0.09	Moderate
Rainfall (RR)	+0.06	−0.02	Low
Sunshine (ss)	+0.07	−0.03	Low
Minimum Temperature (Tn)	+0.04	−0.01	Low
Average Temperature (Tavg)	−0.11	+0.03	Redundant

Table 3 presents the mean degradation in predictive performance, expressed as changes in RMSE (ΔRMSE) and explained variance (ΔR^2), after permuting all derived features related to each variable. Larger ΔRMSE and more negative ΔR^2 indicate higher importance.

The results reveal a clear climatic hierarchy in dengue dynamics. Relative humidity (RH) and maximum temperature (Tx) emerge as the most influential predictors, with ΔRMSE values of 0.66 and 0.57 and corresponding ΔR^2 declines of −0.23 and −0.20. These findings are biologically consistent: humidity governs adult *Aedes aegypti* survival, feeding frequency, and viral competence, while temperature modulates both mosquito metabolism and viral replication speed. The model's reliance on these two parameters, particularly their 2–3-month smoothed and anomaly forms, reflects the delayed but strong climatic control over outbreak onset.

The autoregressive dengue incidence contributes moderately (ΔRMSE = 0.26; $\Delta R^2 = -0.09$), confirming the persistence of local transmission independent of climate. This variable captures endogenous epidemic inertia, meaning that infection rates in previous months strongly influence subsequent case counts through sustained human-vector contact networks.

Rainfall (RR), sunshine (ss), and minimum temperature (Tn) show smaller but non-negligible effects. Rainfall provides breeding habitats yet becomes less predictive at monthly scale due to nonlinear effects such as wash-out during heavy precipitation. Sunshine acts indirectly by shaping temperature and humidity regimes, while minimum temperature primarily ensures baseline vector survival. In contrast, average temperature (Tavg) yields slightly negative ΔRMSE and positive ΔR^2, suggesting redundancy with Tx and Tn and serving mainly as a stabilizing but non-informative feature.

Taken together, the results demonstrate that the TA-LSTM captures a hierarchical sensitivity, ie.: strong external forcing by humidity and temperature; endogenous persistence of infection; and weaker secondary modulation by rainfall and radiation.

This structure aligns closely with entomological and epidemiological theory for tropical dengue systems. The dominance of humidity and temperature highlights the climatic envelope that enables vector proliferation and viral amplification, whereas autoregressive dynamics account for short-term epidemic continuity.

From an operational standpoint, this interpretation indicates that early-warning systems in Lampung can remain effective using a compact predictor set centered on humidity, temperature, and recent incidence history, reducing data dependency without sacrificing model accuracy.

4. CONCLUSION

This study set out to build a climate-informed, data-efficient early-warning model for monthly dengue in Lampung. We first established lead–lag structure (rainfall and temperature lead incidence by ~2–3 months; incidence persists ~2 months), which motivated the use of lagged inputs. We then compared three recurrent architectures (LSTM, Stacked LSTM, and LSTM with Temporal Attention) and tuned their units by a compact Genetic Algorithm. Across generations, performance improved with historical context; the TA-LSTM with 37 units emerged as the best specification (Final Best RMSE = 0.6429), slightly outperforming a wider single-layer LSTM and clearly surpassing the stacked model.

For operational use, we adopt a lag-2 deployment to respect reporting delays: at the end of month t, the system predicts next month $(t+1)$ incidence using data from $t-1$ and $t-2$ (current month data are still being compiled). The output is a single predicted number (per 100,000) that authorities can act upon immediately for this month's interventions (e.g., inventory checks, targeted vector control, risk communication) ahead of the forecast month. This simple workflow keeps the model aligned with the existing data ecosystem and enables direct, timely decision support.

The analytical procedure presented in this study can be applied in other provinces because it is based on a general sequence-modeling approach that uses lagged epidemiological and climatic covariates as inputs for forecasting dengue incidence. Although the workflow itself is transferable, the resulting model parameters cannot be directly used outside the region where they were trained. This is because the lagged incidence and climate variables reflect the data-generating mechanisms that are specific to each province. These mechanisms include local climatic patterns, mosquito ecology, patterns of human movement, land-use characteristics and administrative reporting systems, all of which shape the temporal dependence between climate variability and dengue transmission. For this reason, deploying the method in a new province requires retraining the model with that province's historical data so that the learned temporal relationships represent its own transmission dynamics. The procedure remains reproducible in any setting that maintains consistent monthly dengue and climate records, and future work will extend this framework to multi-provincial or hierarchical modeling to assess external validity and identify potential shared structures across regions.

ACKNOWLEDGEMENTS

The authors would like to express their sincere gratitude to the Institut Teknologi Sumatera (Itera) for providing financial support under the support of Hibah Penelitian Berbasis Kepakaran Institut Teknologi Sumatera the Research Contract Number 1998aq/IT9.2.1/PT.01.03/2025. Special thanks are also extended to the Lampung Provincial Health Office (Dinas Kesehatan Provinsi Lampung) and the Meteorological, Climatological, and Geophysical Agency (BMKG) for their invaluable assistance in providing dengue surveillance and climate data used in this research.

5. REFERENCES

[1] Y. L. Hii, J. Rocklöv, N. Ng, C. S. Tang, F. Y. Pang, and R. Sauerborn, "Climate variability and increase in intensity and magnitude of dengue incidence in Singapore," *Glob. Health Action*, vol. 2, p. 10.3402/gha.v2i0.2036, Nov. 2009, doi: 10.3402/gha.v2i0.2036.

[2] "Dengue." Accessed: Oct. 18, 2025. [Online]. Available: https://www.who.int/news-room/fact-sheets/detail/dengue-and-severe-dengue

[3] Z. Liu *et al.*, "The effect of temperature on dengue virus transmission by Aedes mosquitoes," *Front. Cell. Infect. Microbiol.*, vol. 13, Sept. 2023, doi: 10.3389/fcimb.2023.1242173.

[4] Y. Wang *et al.*, "Impact of climate change on dengue fever epidemics in South and Southeast Asian settings: A modelling study," *Infect. Dis. Model.*, vol. 8, no. 3, pp. 645–655, Sept. 2023, doi: 10.1016/j.idm.2023.05.008.

[5] N. Nuraini, I. S. Fauzi, M. Fakhruddin, A. Sopaheluwakan, and E. Soewono, "Climate-based dengue model in Semarang, Indonesia: Predictions and descriptive analysis," *Infect. Dis. Model.*, vol. 6, pp. 598–611, 2021, doi: 10.1016/j.idm.2021.03.005.

[6] A. Susilawaty, R. Ekasari, L. Widiastuty, D. R. Wijaya, Z. Arranury, and S. Basri, "Climate factors and dengue fever occurrence in Makassar during period of 2011-2017," *Gac. Sanit.*, vol. 35 Suppl 2, pp. S408–S412, 2021, doi: 10.1016/j.gaceta.2021.10.063.

[7] P. Yushananta and M. Ahyanti, "Pengaruh Faktor Iklim dan Kepadatan Jentik Ae. Aegypti Terhadap Kejadian DBD," *J. Kesehat.*, vol. 5, no. 1, 2014, doi: 10.26630/jk.v5i1.58.

[8] P. Yushananta, "Dengue Hemorrhagic Fever and Its Correlation with The Weather Factor In Bandar Lampung City: Study From 2009-2018," *J. Aisyah J. Ilmu Kesehat.*, vol. 6, no. 1, p. 117, Mar. 2021, doi: 10.30604/jika.v6i1.452.

[9] V. G. Ramachandran, P. Roy, S. Das, N. S. Mogha, and A. K. Bansal, "Empirical model for estimating dengue incidence using temperature, rainfall, and relative humidity: a 19-year retrospective analysis in East Delhi," *Epidemiol. Health*, vol. 38, p. e2016052, Nov. 2016, doi: 10.4178/epih.e2016052.

[10] A. Anwar and J. Ariati, "Model Prediksi Kejadian Demam Berdarah Dengue (DBD) Berdasarkan Faktor Iklim di Kota Bogor, Jawa Barat," *Indones. Bull. Health Res.*, vol. 42, no. 4, p. 20092, 2014, doi: 10.22435/bpk.v42i4.

[11] D. Perwitasari and Y. Ariati, "Model Prediksi Demam Berdarah Dengue Dengan Kondisi Iklim Di Kota Yogyakarta," *Indones. J. Health Ecol.*, vol. 14, no. 2, pp. 124–135, 2015.

[12] "Peringatan Dini DBD – DKI Jakarta | Informasi Iklim BMKG." Accessed: Oct. 18, 2025. [Online]. Available: https://iklim.bmkg.go.id/id/dbdklim/

[13] "DBDKlim Bali – Stasiun Klimatologi Bali." Accessed: Oct. 18, 2025. [Online]. Available: https://staklim-bali.bmkg.go.id/?page_id=2708

[14] N. A. Lestari, R. Tyasnurita, R. A. Vinarti, and W. Anggraeni, "Long Short-Term Memory forecasting model for dengue fever cases in Malang regency, Indonesia," *Procedia Comput. Sci.*, vol. 197, pp. 180–188, Jan. 2022, doi: 10.1016/j.procs.2021.12.131.

[15] A. Sebastianelli *et al.*, "A reproducible ensemble machine learning approach to forecast dengue outbreaks," *Sci. Rep.*, vol. 14, no. 1, p. 3807, Feb. 2024, doi: 10.1038/s41598-024-52796-9.

[16] Islam Jahirul, Frentiu Francesca D., Devine Gregor J., Bambrick Hilary, and Hu Wenbiao, "A State-of-the-Science Review of Long-Term Predictions of Climate Change Impacts on Dengue Transmission Risk," *Environ. Health Perspect.*, vol. 133, no. 5, p. 056002, doi: 10.1289/EHP14463.

[17] M. A. Morid, O. R. L. Sheng, and J. Dunbar, "Time Series Prediction Using Deep Learning Methods in Healthcare," *ACM Trans Manage Inf Syst*, vol. 14, no. 1, p. 2:1-2:29, Jan. 2023, doi: 10.1145/3531326.

[18] X. Shi, Z. Chen, H. Wang, D.-Y. Yeung, W. Wong, and W. Woo, "Convolutional LSTM Network: A Machine Learning Approach for Precipitation Nowcasting," Sept. 19, 2015, *arXiv*: arXiv:1506.04214. doi: 10.48550/arXiv.1506.04214.

[19] X. Chen and P. Moraga, "Dengue forecasting and outbreak detection in Brazil using LSTM: integrating human mobility and climate factors," June 19, 2025, *medRxiv*. doi: 10.1101/2025.03.02.25323168.

[20] S. R. A. Sofian, Sudarti, and R. D. Handayani, "Analisis Korelasi Curah Hujan dan Produktivitas Tanaman Hasil Pertanian Kabupaten Jember," *J. Pendidik. MIPA*, vol. 12, no. 2, pp. 287–293, June 2022, doi: 10.37630/jpm.v12i2.612.

[21] M. A. Majeed, H. Z. M. Shafri, Z. Zulkafli, and A. Wayayok, "A Deep Learning Approach for Dengue Fever Prediction in Malaysia Using LSTM with Spatial Attention," *Int. J. Environ. Res. Public. Health*, vol. 20, no. 5, p. 4130, Jan. 2023, doi: 10.3390/ijerph20054130.